Characteristics of short period secondary microseisms (SPSM) in Taiwan: The influence of shallow ocean strait on SPSM

Ying-Nien Chen,[1] Yuancheng Gung,[2] Shuei-Huei You,[2] Shu-Huei Hung,[2] Ling-Yun Chiao,[1] Tzu-Ying Huang,[2] Yen-Ling Chen,[3] Wen-Tzong Liang,[4] and Sen Jan[1]

Received 24 November 2010; revised 7 January 2011; accepted 13 January 2011; published 23 February 2011.

[1] Taking advantage of a unique opportunity provided by a dense array of coastal short-period seismic stations and the diverse bathymetry around Taiwan, we examine how the long-range coherent ambient noises are influenced by surrounding ocean settings using the cross-correlation functions (CCFs) between pairs of stations. The effective energy of the CCFs derived from three components of short-period seismometer data falls within the frequency range of the short period secondary microseism (SPSM). The spatial variations mapped from the amplitude asymmetry of CCFs and source migration images evidently demonstrate that the SPSM strengths are closely linked to the drastic changes in offshore ocean characteristics and result in much stronger SPSM in the shallow and narrow Taiwan Strait than in deep open seas of eastern Taiwan. The temporal variations of the CCF strengths exhibit very good correlations with the wind speeds and wave heights, explicitly indicating the observed SPSM is dominated by local sources generated from wind-driven ocean waves around offshore Taiwan. **Citation:** Chen, Y.-N., Y. Gung, S.-H. You, S.-H. Hung, L.-Y. Chiao, T.-Y. Huang, Y.-L. Chen, W.-T. Liang, and S. Jan (2011), Characteristics of short period secondary microseisms (SPSM) in Taiwan: The influence of shallow ocean strait on SPSM, *Geophys. Res. Lett.*, *38*, L04305, doi:10.1029/2010GL046290.

1. Introduction

[2] It has been shown that the cross-correlation function (CCF) of continuous records from two wave sensors resembles the elastice impulse response between them [e.g., *Weaver and Lobkis*, 2001, 2002; *Shapiro and Camille*, 2004; *Snieder*, 2004]. Theoretically, in a fully diffusive wave field, the causal (time positive portion) and acausal (time negative portion) signals of the derived CCFs are identical in both their phases and amplitudes. In the application to seismic data, prior to cross-correlation, various noramalizations applied to raw data are indispensible in order to suppress non-diffusive signals such as earthquakes and instrumental irregularities. The phase symmetry with respect to zero time lag is usually fairly attained in the resulting CCFs, and the violation of phase symmetry is mostly related to errors of the internal clock of seismometers [e.g., *Lukac et al.*, 2009; *You et al.*, 2010]. On the other hand, compatible amplitudes for causal and acausal signals are less common, and it is due to the fact that the source strengths of background noises are not spatially homogeneous. Because the causal and acausal signals of CCFs are mainly excited by the sources from opposite directions along the line of the station pair, the characteristics of CCF amplitudes has become a useful means to explore the source heterogeneities of ambient noises [e.g., *Gu et al.*, 2007; *Brzak et al.*, 2009].

[3] Seismic ambient noise exists across a wide frequency band, in which microseisms are the most common signals in seismograms at periods between ~3 to 20 seconds. Microseisms are primarily generated by the coupling between ocean waves and seafloor [e.g., *Longuet-Higgins*, 1950; *Cessaro*, 1994]. While some studies on the amplitude asymmetry of CCFs suggest that short-period microseisms (<10 seconds) are mostly excited in the coastal area [e.g., *Stehly et al.*, 2006; *Yang and Ritzwoller*, 2008], other investigation found that they could be effectively generated by resonance of the compression waves at favorable depth in deep oceans as well [*Kedar et al.*, 2008].

[4] The island of Taiwan is located on the arc-continent collision boundary between the Eurasia plate and Philippine Sea plate. Owing to this complex tectonic setting, the north-south trending mountain ranges run through the central Taiwan and divide the island into the western and eastern parts surrounded by very diverse bathymetry as shown in Figure 1a. The seafloor morphology off southern and eastern Taiwan is strongly associated with the juxtaposition of oblique collision and subduction between two plates and the water depth steeply increases off the coast. In contrast, to the western and northern Taiwan the narrow Taiwan Strait basin, part of the passive South China continental margin, has relatively flat and much shallower bathymetry with an average water depth of about 70 meters only [*Liu et al.*, 1998].

[5] In Taiwan, most seismic stations are deployed near the coasts. Not surprisingly, the recorded background seismic noise level is much higher than the global average for periods less than ~8 s [*Lin et al.*, 2010]. Although the energetic background noise may obscure micro earthquake signals, it turns out to be an advantage in the implementation of ambient noise tomography [*You et al.*, 2010]. Moreover, the combination of dense coastal stations and diverse offshore morphology provides a unique opportunity to explore how the long-range coherent ambient noises are influenced by the fluctuations in offshore settings.

[6] In this study, we analyze CCFs derived from three components of data recorded by short-period seismic stations of the Central Weather Bureau Seismic Network (CWBSN). The major energy of the resulting CCFs falls within the

[1]Institute of Oceanography, National Taiwan University, Taipei, Taiwan.
[2]Department of Geosciences, National Taiwan University, Taipei, Taiwan.
[3]Seismological Center, Central Weather Bureau, Taipei, Taiwan.
[4]Institute of Earth Sciences, Academia Sinica, Taipei, Taiwan.

0094-8276/11/2010GL046290

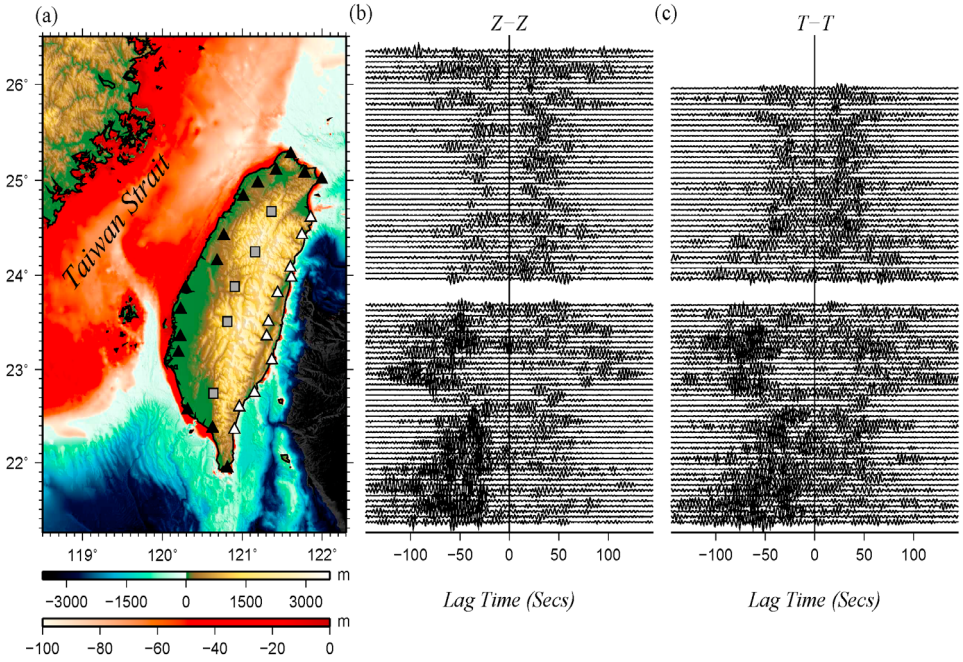

Figure 1. (a) Map of the study region and stations used. The west and east coast stations are denoted by black and white triangles, respectively. The inland stations are denoted by gray squares. The topography and bathymetry are also shown as defined by the color bars. Different color scale is used for the depth range between 0 and 100m to better illustrate the shallow bathymetry in the Taiwan Strait. (b) CCFs derived from the vertical component. The causal and acausal signals of CCFs are related to energy coming from the inland and coastal direction, respectively. The CCFs (top) from stations along the east coast and (bottom) for the stations from the west coast. The amplitude of each trace is normalized by the smaller peak amplitude between the corresponding causal and acausal signals. (c) Same as Figure 1b, except for the transverse component.

period range of about 2 to 6 seconds. Microseisms within this frequency band are known as short period secondary microseism (SPSM) [*Stephen et al.*, 2003; *Bromirski et al.*, 2005].

[7] We characterize the spatiotemporal property of the SPSM intensity by the amplitude asymmetry of CCFs and their source distributions in offshore regions determined by a migration imaging method. Results from both approaches clearly demonstrate that SPSM are much stronger in shallow water settings. Moreover, the close connection between the long-range coherent seismic ambient noises and atmosphere perturbations is manifested by the excellent temporal coherence between the monthly-averaged CCF amplitudes and the wind speeds and wave heights.

2. Data

[8] Among a total of 78 short-period CWBSN stations distributed over the island, we select 31 representative stations for this study; 26 of them are located near the coastal area with an approximately uniform spacing along the circum-island coast line, and the rest situated in the inland area along the Central Mountain Ranges (Figure 1a).

[9] It is well known that noise-derived CCFs are dominated by fundamental mode Rayleigh waves for the vertical (Z) and radial components, and by Love waves for the transverse (T) component [e.g., *Camille and Paul*, 2003]. To take both wave types into account, we derive CCFs of the Z-Z and T-T components using three components of continuous records in the year 2006. The main purpose of this study is to examine how the noise excitations are influenced by different offshore settings, hence, only the station pairs composed of one coastal and one inland station are used in the CCF analysis.

[10] Figure 2 shows the spectral contents of the resulting CCFs on the T-T and Z-Z components which both concentrate within the narrow SPSM band at the peaks of around 4 seconds. (See auxiliary material for instrument response and details on data processing.)[1]

3. Spatiotemporal Characteristics of SPSM

3.1. Spatial Variations of CCF Amplitude Asymmetry

[11] We first explore the spatial variations of the noise excitations using the amplitude asymmetry of annual CCFs. Only the CCFs with effective emergence of the empirical Green's function (EGF) are used in this analysis. 86 pairs of the CCFs from the Z-Z components and 79 pairs from the T-T components meet the selection criterion (see auxiliary material), and are shown in Figures 1b and 1c, respectively. It is fairly clear that the CCFs obtained with one of the paired stations from the west coast show strong amplitude asymmetry, while the asymmetry is much weaker for the CCFs derived from the eastern coastal stations. It's worth mentioning that seismicity in Taiwan is very active along the east coast and very quiet on the west coast [e.g., *Wu and Rau*, 1998]. The above results suggest that transient

[1] Auxiliary materials are available in the HTML. doi:10.1029/2010GL046290.

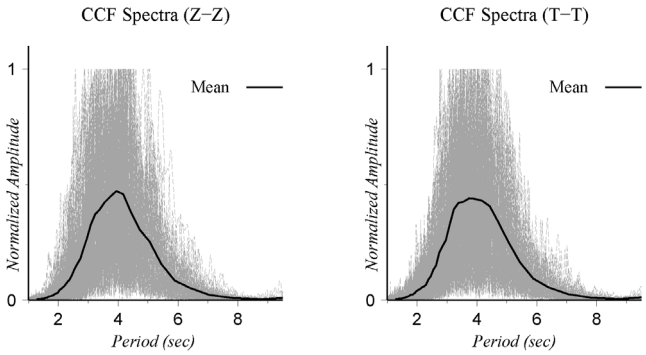

Figure 2. Amplitude spectra of the noise-derived CCFs for the Z-Z and T-T components. All the spectra are normalized to emphasize their frequency contents. The gray lines show the spectra of annual CCF stacks for all the available pairs, and black curves represent the corresponding mean spectra.

earthquake signals have little contribution to the emergence of EGFs after raw data normalization.

[12] The amplitude asymmetry is further quantified by taking the ratio of the peak amplitudes of a CCF in one of the causal or acausal signals excited from the coastal direction to that in the other signal excited from the inland direction. The results are displayed as vectors on the locations of coastal stations, with their lengths proportional to the amplitude ratios and direction to the energy flow along the lines of station pairs. Results from Rayleigh waves (Figure 3a) and Love waves (Figure 3b) demonstrate very similar patterns wherein the SPSM excitations from the Taiwan Strait and northern coast are much stronger than those from the eastern and southern coasts. The color images of the offshore area in Figure 3 are the lateral variations of the SPSM intensity resulting from the noise source migration (see Section 3.2).

[13] We have also conducted a similar experiment using 10 coastal broad-band stations to ensure that the above observations on the spectral content and amplitude asymmetry are not biased by the band-limited response of short-period stations (see auxiliary material).

3.2. Spatial Variations of SPSM Sources From Migration Imaging Method

[14] To further look into the spatial distribution of noise sources, we implement the migration imaging method [*Brzak et al.*, 2009]. Briefly speaking, with the noise-derived 2-D surface wave models [*Chen et al.*, 2009] in the Taiwan island and an average wave velocity for the oceanic area, the excitations of potential SPSM sources are evaluated based upon the strength of cross-correlated signals among all available station pairs, and the whole offshore area in Figure 1 are estimated at every 0.05 by 0.05 degree grid cells.

[15] All the annual CCFs on the Z-Z and T-T components are used for the source migration analysis, and the lateral variations of the resulting SPSM intensities are presented as relative perturbations with respect to the regional average (Figure 3). The distribution of source intensity is consistent with the pattern of the CCF amplitude asymmetry, indicating that the SPSM are stronger in the west and north offshore Taiwan. (More details on the migration imaging method and the stability test are given in the auxiliary material.)

3.3. Temporal Variations of CCF Amplitudes and Their Correlation to Wind Speeds and Wave Heights

[16] The temporal variations of overall CCF amplitudes are estimated by the relative differences of the average peak amplitudes between individual monthly stacks and annual stacks. We then compare the monthly variations of CCF amplitudes with wind speeds and offshore ocean wave heights for the same time period to further demonstrate their close relationships. The monthly means of 20 island-wide coastal meteorological observatories and 6 offshore buoys in 2006 are used to derive the temporal variations of wind speeds and wave heights with respect to their annual means (see auxiliary material for data sources of wind speeds and wave heights). The comparison is shown Figure 4, which reveals strong positive correlations among the variations in CCF amplitudes, wind speeds and ocean wave heights.

4. Discussions and Conclusions

[17] We have examined the spatiotemporal properties of SPSM around the offshore Taiwan using noise-derived CCFs. Both the spatial and temporal variations of the SPSM excitations exhibit characteristic features which are likely linked to the diverse offshore settings and monsoon migration in Taiwan.

[18] The strong east–west asymmetry in SPSM intensity is evidently demonstrated by the CCF amplitude ratios and migration images, and such pattern matches very well with the corresponding drastic changes of seafloor morphology and ocean characteristics surrounding Taiwan shown in

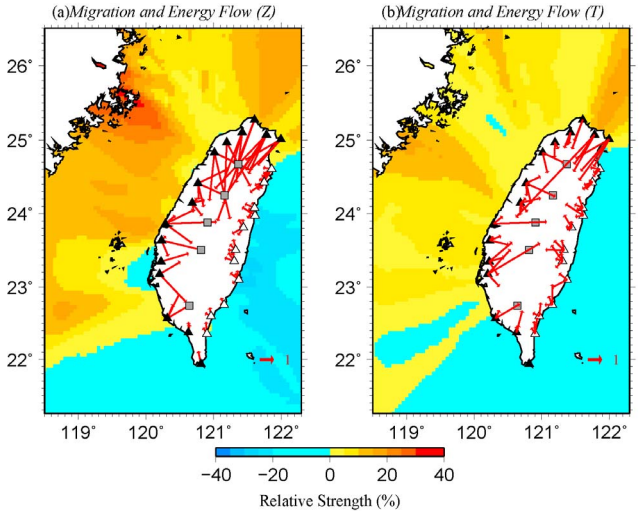

Figure 3. Results of migration imaging of SPSM strengths and relative peak amplitudes of the annual CCF stacks for the (a) Z-Z and (b) T-T components. The relative strengths of CCFs are shown as vectors on the locations of coastal stations, with their lengths proportional to the amplitude ratios (scale shown in the lower-right corner of each panel) and directions to the energy flow along the line of station pairs (see text for details). The results of migration images are expressed as perturbations with respect to the regional average.

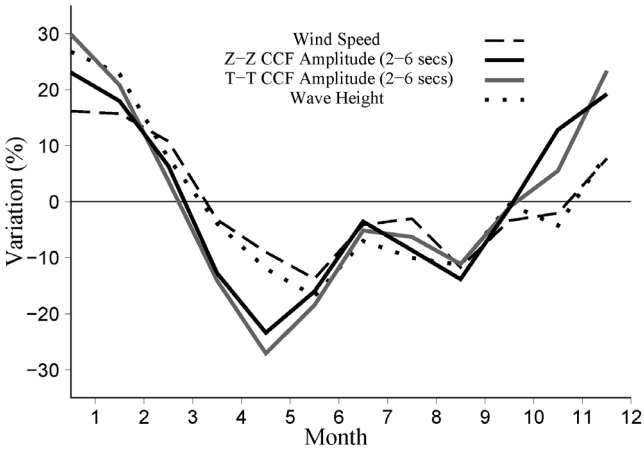

Figure 4. Comparison of the temporal variations between wind speeds and CCF amplitudes. The dashed and dot lines represent the variations of overall monthly wind speeds and wave heights with respect to their annual averages. The solid lines are the variations of overall CCF amplitudes for the Z-Z component (black line) and T-T component (gray line). Only either the causal or acausal CCF signals corresponding to the directions of energy flow that point from the coastal stations to inland stations are taken into account.

Figure 1a. Although the shallower water depth and the narrow ocean strait are plausible causes for the stronger SPSM in the Taiwan Strait and northern offshore, there are other possibilities to explain our observations, such as the wave heights or frequency content of ocean waves.

[19] We first examine the wave heights in offshore Taiwan from data recorded by six offshore buoys in the year 2006 (see Figure S4 in the auxiliary material). Wave heights recorded in the northern end and southern end of Taiwan are relatively higher (106 cm) and lower (63 cm), respectively, consistent with the observed SPSM intensity. However, there is no significant difference in annual means of wave heights (~90 cm) between the west and east coasts.

[20] Second, there might be a doubt that the observed east–west asymmetry in SPSM excitations is merely a consequence of the difference in frequency contents between waves in the Taiwan Strait and the eastern open sea, as it is well known that the frequency of ocean waves generated in a small ocean basin is higher than in the deep open sea. This could be verified by comparing the spectra of CCF signals from the east and west coasts, since waves with different frequencies would leave their signatures on the resulting secondary microseisms. The comparison made in Figure S5 of the auxiliary material shows that the frequency contents of the signals from both coasts are very similar. Another line of evidence is provided by the strong temporal correlation between CCF amplitudes and local wind speeds (Figure 4). It implies that the observed SPSM are dominated by waves generated locally in offshore area, and the distant lower frequency ocean swells in deep sea should have little influence.

[21] Given the above arguments, we thus propose that much of the observed spatial variations in SPSM intensity are related to the contrasting offshore settings between the east and west coasts. Stronger excitations take place in the narrow Taiwan Strait where water depth is very shallow, while the excitations are relatively weak in the eastern offshore area, an open sea with water depth increases rapidly off the coast.

[22] The correlation between bathymetry and excitation strength is in agreement with the generation mechanism of microseisms. Because ocean wave energy is transferred to microseisms through the interaction of ocean swells with a shoaling ocean bottom, and the transferred energy decays quickly with increasing water depth, reaching to nearly zero at the depth equal to half the wavelength. The observed SPSM correspond to ~8 second ocean waves, whose wavelength would be ~80 meters. As shown in Figure 1a, the water depth of a large portion of the Taiwan Strait is less than 40 meters, and such shallow bathymetry may enhance the nonlinear interactions of waves through the stronger bottoming friction, and introduce more effective SPSM excitation.

[23] The narrow Taiwan Strait might be a privileged place for the generation of secondary microseisms as well. Because secondary microseisms are induced by nonlinear interactions between oppositely traveling ocean waves of similar wavelengths [e.g., *Longuet-Higgins*, 1950], their excitations should be more vigorous through the coastal reflections of ocean waves from both sides of the strait. Furthermore, the decay of ocean waves due to geometrical spreading in a confined basin like the Taiwan Strait is much less than that in an open ocean, and this could be another possible cause for the observed stronger SPSM in the west offshore of Taiwan.

[24] On the other hand, the strong temporal correlation among CCF amplitudes, wind speeds and wave heights confirms that the SPSM strength is closely related to the local wind fields and ocean waves [e.g., *Bromirski and Duennebier*, 2002; *McNamara and Buland*, 2004; *Gerstoft and Tanimoto*, 2007; *Traer et al.*, 2008]. It is known that the wind fields over Taiwan are strictly tied to the East Asia monsoon system, in which the northeast monsoon commences in September, prevails from October to January, and weakens continuously thereafter; the southwest monsoon only prevails in June to August, and is much weaker than the northeast monsoon. The observed temporal variations of SPSM strength can thus be well explained by the seasonal migration of the two monsoons.

[25] **Acknowledgments.** This research is supported by the National Science Council of Taiwan under the grant NSC 99-2116-M-002-027 and NSC 99-2611-M-002-009. We wish to thank the operators of the CWB, BATs, and DBAR for providing high-quality seismic, buoy and wind speed data. Comments from two anonymous reviewers and discussions with Prof. Chen-fen Huang have improved this work considerably. English editing assistance provided through Taiwan Earthquake Research Center (TEC) is acknowledged. M. E. Wysession thanks two anonymous reviewers.

References

Bromirski, P. D., and F. K. Duennebier (2002), The near-coastal microseism spectrum: Spatial and temporal wave climate relationships, *J. Geophys. Res.*, *107*(B8), 2166, doi:10.1029/2001JB000265.

Bromirski, P. D., F. K. Duennebier, and R. A. Stephen (2005), Mid-ocean microseisms, *Geochem. Geophys. Geosyst.*, *6*, Q04009, doi:10.1029/2004GC000768.

Brzak, K., Y. J. Gu, A. Ökeler, M. Steckler, and A. Lerner-Lam (2009), Migration imaging and forward modeling of microseismic noise sources near southern Italy, *Geochem. Geophys. Geosyst.*, *10*, Q01012, doi:10.1029/2008GC002234.

Camille, M., and A. Paul (2003), Long-range correlations in the diffuse seismic coda, *Science*, *299*, 547–549, doi:10.1126/science.1078551.

Cessaro, R. K. (1994), Sources of primary and secondary microseisms, *Bull. Seismol. Soc. Am.*, *84*, 142–148.

Chen, Y., Y. Gung, S. You, L. Chiao, W. Liang, and C. Lin (2009), On Short Period Ambient Noise of Taiwan (1) Ambient Noise Tomography (2) Probing Source of Ambient Noise, *Eos Trans. AGU*, *90*(52), Fall Meet. Suppl., Abstract S53A-1460.

Gerstoft, P., and T. Tanimoto (2007), A year of microseisms in southern California, *Geophys. Res. Lett.*, *34*, L20304, doi:10.1029/2007GL031091.

Gu, Y. J., C. Deblanko, A. Lener-Lam, K. Brzak, and M. Steckler (2007), Probing the source of ambient seismic noise near the coasts of southern Italy, *Geophys. Res. Lett.*, *34*, L22315, doi:10.1029/2007GL031967.

Kedar, S., M. Longuet-Higgins, F. Webb, N. Graham, R. Clayton, and C. Jones (2008), The origin of deep ocean microseisms in the North Atlantic Ocean, *Proc. R. Soc. A*, *464*(2091), 777–793, doi:10.1098/rspa.2007.0277.

Lin, C. R., B. Y. Kuo, W. T. Liang, W. C. Chi, Y. C. Huang, J. Collins, and C. Y. Wang (2010), Ambient noise and teleseismic signals recorded by ocean-bottom seismometers offshore eastern Taiwan, *Terr. Atmos. Oceanic Sci.*, *21*, 743–755, doi:10.3319/TAO.2009.09.14.01(T).

Liu, C. S., S. Y. Liu, S. E. Lallemand, N. Lundberg, and D. L. Reed (1998), Digital Elevation model offshore Taiwan and its tectonic implication, *Terr. Atmos. Oceanic Sci.*, *9*, 705–738.

Longuet-Higgins, M. S. (1950), A theory of the origin of microseisms, *Philos. Trans. R. Soc. London, Ser. A*, *243*, 1–35, doi:10.1098/rsta.1950.0012.

Lukac, M., P. Davis, R. Claytion, and D. Estrin (2009), Recovering temporal integrity with data driven time synchronization, in *Proceedings of the 8th International Conference on Information Processing in Sensor Networks*, pp. 61–72, Univ. Trier, Trier, Germany.

McNamara, D. E., and R. P. Buland (2004), Ambient noise levels in the continental United States, *Bull. Seismol. Soc. Am.*, *94*, 1517–1527, doi:10.1785/012003001.

Shapiro, N. M., and M. Camille (2004), Emergence of broadband Rayleigh waves from correlations of the ambient seismic noise, *Geophys. Res. Lett.*, *31*, L07614, doi:10.1029/2004GL019491.

Snieder, R. (2004), Extracting the Green's function from the correlation of coda waves: A derivation based on stationary phase, *Phys. Rev. E*, *69*, 046610, doi:10.1103/PhysRevE.69.046610.

Stehly, L., M. Camille, and N. M. Shapiro (2006), A study of the seismic noise from its long-range correlation properties, *J. Geophys. Res.*, *111*, B10306, doi:10.1029/2005JB004237.

Stephen, R. A., F. N. Spiess, J. A. Hildebrand, J. A. Orcutt, K. R. Peal, F. L. Vernon, and F. B. Wooding (2003), Ocean Seismic Network Pilot Experiment, *Geochem. Geophys. Geosyst.*, *4*(10), 1092, doi:10.1029/2002GC000485.

Traer, J., P. Gerstoft, P. D. Bromirski, W. S. Hodgkiss, and L. A. Brooks (2008), Shallow-water seismoacoustic noise generated by tropical storms Ernesto and Florence, *J. Acoust. Soc. Am.*, *124*, doi:10.1121/1.2968296.

Weaver, R. L., and O. I. Lobkis (2001), On the emergence of the Green's function in the correlations of a diffuse field, *J. Acoust. Soc. Am.*, *110*, 3011–3017, doi:10.1121/1.1417528.

Weaver, R. L., and O. Lobkis (2002), On the emergence of the Green's function in the correlations of a diffuse field: Pulse-echo using thermal phonons, *Ultrasonics*, *40*, 435–439, doi:10.1016/S0041-624X(02)00156-7.

Wu, F. T., and R.-J. Rau (1998), Seismotectonics and identification of potential seismic source zone in Taiwan, *Terr. Atmos. Oceanic Sci.*, *9*(4), 739–754.

Yang, Y., and M. H. Ritzwoller (2008), Characteristics of ambient seismic noise as a source for surface wave tomography, *Geochem. Geophys. Geosyst.*, *9*, Q02008, doi:10.1029/2007GC001814.

You, S.-H., Y. Gung, L.-Y. Chiao, Y.-N. Chen, C.-H. Lin, W.-T. Liang, and Y.-L. Chen (2010), Multi-scale ambient noise tomography of short period Rayleigh waves across northern Taiwan, *Bull. Seismol. Soc. Am.*, *100*, 3165–3173, doi:10.1785/0120090394.

Y.-L. Chen, Seismological Center, Central Weather Bureau, 64, Gongyuan Rd., Taipei 10048, Taiwan.

Y.-N. Chen, L.-Y. Chiao, and S. Jan, Institute of Oceanography, National Taiwan University, No. 1, Sec. 4 Roosevelt Rd., Taipei 106, Taiwan.

Y. Gung, T.-Y. Huang, S.-H. Hung, and S.-H. You, Department of Geosciences, National Taiwan University, No. 1, Sec. 4 Roosevelt Rd., Taipei 106, Taiwan. (ycgung@ntu.edu.tw)

W.-T. Liang, Institute of Earth Sciences, Academia Sinica, PO Box 1-55, Taipei 115, Taiwan.